Chapter 2
Electrospray Ionization Traveling Wave Ion Mobility Spectrometry Mass Spectrometry for the Analysis of Plant Phenolics: An Approach for Separation of Regioisomers

Fereshteh Zandkarimi, Samanthi Wickramasekara, Jeff Morre, Jan F. Stevens and Claudia S. Maier

Abstract The use of ion-mobility spectrometry (IMS) coupled to mass spectrometry (IMS–MS) for biomolecule analyses has steadily increased over the past two decades, and is now applied to both proteomic and metabolomic investigations. This chapter describes the application of traveling-wave ion-mobility spectrometry–mass spectrometry (TWIMS–MS) to the analysis of a selection of bioactive phytochemicals used in dietary supplements. Applications include the analysis of grape seed proanthocyanidins and the structural characterization of bioactive constituents of dietary supplements using TWIMS-MS in conjunction with tandem mass spectrometry. We also discussed is the application of TWIMS-MS for the gas-phase mobility separation of structural isomers and the estimation of collision cross sections for a small selection of phenolic compounds from hop. Recent applications of IMS–MS to a broad range of biomolecule measurements have demonstrated that IMS–MS has emerged as a powerful analytical technique capable of providing the separation space necessary to analyze highly complex samples. We give a perspective on emerging applications of IMS–MS for small molecule and biopolymer applications. The combination of devices that allow real-time monitoring of living systems using IMS–MS is an exciting avenue of facilitating system-biology experiments. The future of IMS–MS is bright and full of opportunities.

C. S. Maier (✉) · F. Zandkarimi · S. Wickramasekara · J. Morre
Department of Chemistry, Oregon State University, Corvallis, OR 97331, USA
e-mail: Claudia.maier@oregonstate.edu

S. Wickramasekara · J. Morre · J. F. Stevens · C. S. Maier
Environmental Health Sciences Center, Oregon State University, Corvallis, OR 97331, USA

J. F. Stevens
Department of Pharmaceutical Sciences, Oregon State University, Corvallis, OR 97331, USA

Linus Pauling Institute, Oregon State University, Corvallis, OR 97331, USA

D. R. Gang (ed.), *50 Years of Phytochemistry Research*,
Recent Advances in Phytochemistry 43, DOI 10.1007/978-3-319-00581-2_2,

2.1 Introduction

There is increasing evidence that plant phenolics have health benefits which may, at least partially, stem from their antioxidant and radical scavenging activity [1–3]. Considering the increasing interest in plant phenolics as nutraceuticals, comprehensive profiling methods for plant extracts are highly needed. We report on the characterization of plant phenolics using traveling-wave ion-mobility spectrometry–mass spectrometry (TWIMS–MS) and emphasize the structural analysis of plant secondary metabolites that are commonly found in over-the-counter dietary supplements.

The use of ion-mobility spectrometry (IMS) coupled to mass spectrometry (IMS–MS) for biomolecule analyses has steadily increased since the 1990s. Many applications describe IMS–MS for studying peptides and proteins and their folding behaviors in the gas phase [4–10]. IMS–MS has also been used for assessing synthetic polymers [11, 12]. More recently, IMS–MS has been described as a powerful addition to the arsenal of tools for the structural analysis of small molecules including drugs, metabolites, lipids, carbohydrates, phytochemicals, and other natural products [13–19]. Comprehensive reviews are available that describe in detail the principles and applications of IMS–MS [20–22]. Briefly, in IMS ions are separated according to their charge state, shape, and size. IMS systems function as gas-phase separation devices. IMS uses nondestructive low-energy collisions to separate ions predominately on the basis of ion-neutral collision cross sections. Ion-mobility separations in the gas phase have considerably lower resolution compared to the resolution that can be achieved with modern condensed phase chromatographic separation technologies. However, the separation of ions occurs several orders of magnitudes faster than separations based on liquid chromatographic techniques; ion-mobility separations usually occur on a time scale of milliseconds compared to the seconds to hours in chromatographic separations. MS measurements occur in the microsecond range and, as such, are nested within the IMS experiments [23]. IMS–MS experiments allow real-time separations of the components of complex mixtures and provide access to three-dimensional (3D) analytical information, namely shape, mass, and abundance. The combination of IMS with MS results in two-dimensional plots of drift time (t_d) versus *m/z*. The three-dimensionality of TWIMS–MS datasets is best captured in so-called driftscope images that contain information regarding the drift time (t_d, in ms) and *m/z* values displayed in a nested fashion, t_d as function of (*m/z*), with ion abundances given in a color-coded style. These images enable the extraction of distinct features that otherwise would get lost or overlap in crowed spaces of traditional mass spectra. A unique feature of IMS–MS is the ability to conduct drift time measurements that allow the calculation of collision cross sections (CCSs) for low- and high–molecular-weight molecules and the possible separation of isomeric analytes, which is not possible solely with MS-based techniques [13–15].

IMS–MS systems are available in many different instrument configurations. In the traditional configuration, the drift tube-based IMS device is placed between the ionization source and the mass analyzer [20]. The recent advent of a commercial

IMS–MS system, in which a traveling-wave IMS device has been integrated into a hybrid quadrupole-orthogonal acceleration time-of-flight (TOF) mass spectrometer, opens new possibilities for the structural characterizations of small molecules and biopolymers [24]. In this contribution, we describe the application of TWIMS–MS for the analysis of a selection of bioactive phytochemicals used in dietary supplements. We first give a brief description of the TWIMS–MS instrument used. Then, we discuss several applications of TWIMS–MS: (1) the analysis of a biopolymer mixture, namely grape seed proanthocyanidins; (2) the structural characterization of bioactive constituents of dietary supplements using TWIMS in conjunction with tandem mass spectrometry; and (3) the gas-phase mobility separation of structural isomers and the estimation of collision cross sections for a small selection of phenolic compounds from hop. We conclude with a brief review of recent developments and applications, and provide a perspective on the emerging application of IMS–MS for small molecule and biopolymer applications.

2.2 Ion-Mobility Mass Spectrometry Using an Electrospray Ionization Quadrupole Traveling-Wave Ion-Mobility TOF Instrument

Many different instrument designs have been described that combine IMS with different types of MS analyzers [20]. The availability of a commercial hybrid system that integrates traveling-wave ion-mobility separation with a quadrupole TOF analyzer makes the technology accessible to a wider research community. For the applications described here, we used a Waters Synapt G2 HDMS instrument equipped with an electrospray ionization (ESI) source. This instrument has the following configuration: a quadrupole mass filter, the TriWave™ section consisting of three traveling-wave (T-wave) devices (Trap T-wave, Ion mobility separation (IMS) T-Wave, and Transfer T-wave) and an orthogonal acceleration (oa) TOF analyzer (Fig. 2.1). The traveling-wave IMS device is a radio-frequency (RF) ion guide based on a stack of ring electrodes. The RF voltage confines the ions radially. By applying a continuous series of DC voltage pulses traveling along the stacked ring electrodes, ions are moved through the gas-filled guide. The ability of an ion to travel along with the DC pulse through the gas-filled T-wave ion guide will depend on the ion's size, charge, shape, and the interaction cross section between the ion and background gas. Instrumental parameters that affect the ability of an ion to move with the traveling wave are the amplitude of the wave, the travel velocity of the wave, and the type and pressure of the background gas. Applying an optimized set of parameters, high-mobility ions will travel with the wave and pass through the ion guide faster than ions with low mobility, which roll over the top of the wave and as a result spend more time in the device [24].

The TriWave™ section of this instrument consists of three traveling-wave-enabled stacked ring ion guides. This configuration allows for unique fragmentation experiments (Table 2.1). The trap ion guide is used for the accumulation of ions and

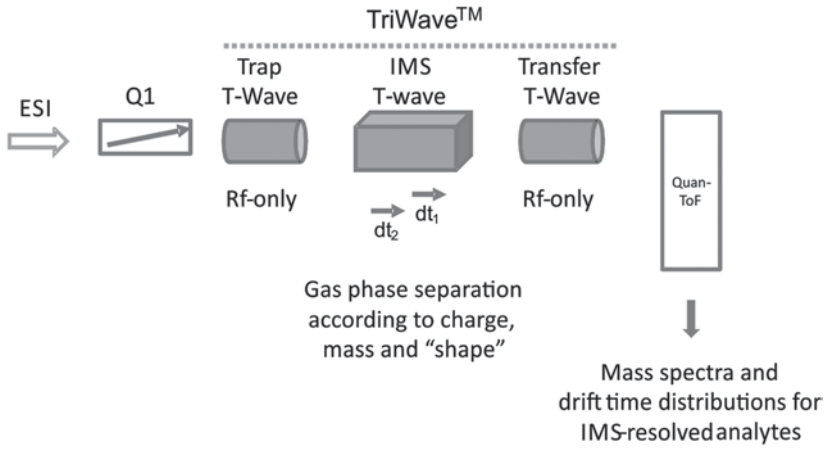

Fig. 2.1 Conceptual diagram of the commercially available TWIMS–MS instrument (Waters Synapt G2 HDMS instrument) operated in the mobility time-of-flight (TOF) mode. This operating mode is used for gas-phase mobility separation of ions in combination with high-resolution mass spectrometry. This mode also enables the extraction of drift times for the estimation of collision cross sections after calibrating the traveling-wave ion-mobility separator. In mobility-TOF mode, the quadrupole (Q1) analyzer is operated in the transmitting mode, the trap and transfer devices serve at radio-frequency (Rf)-only ion guides. *T-wave*, traveling wave; *IMS*, ion mobility spectrometry; *dt*, drift time

release of ions as packets into the ion-mobility separation device. The transfer ion guide conveys the mobility-separated ions to the orthogonal acceleration (oa) TOF analyzer. Fragmentation can take place either in the trap, in the transfer device, or in both devices. A detailed description of the working principle and the design of the traveling-wave ion-mobility separator have been published previously by Giles et al. [24, 25]. Details on the theoretical background on classical IMS–MS and the adaption to traveling TWIMS–MS have also been described in several recent papers [24–27]. In the following sections, we describe the use of TWIMS–MS experiments for the structural characterization of plant phenolics.

2.3 TWIMS–MS Analysis of Biopolymers: Application to Grape Seed Proanthocyanidins

Grape seed extracts have been extensively studied by diverse mass spectrometric techniques. In most cases, the mass spectrometric analyses were accompanied by laborious and extensive chromatography of the highly complex grape seed proanthocyanidin mixtures [28–30]. Considering the current interest in grape seed proanthocyanidins as nutraceuticals in biomedical applications, comprehensive and fast profiling of grape seed extracts is highly desirable. The analysis of proanthocyanidins by ESI–MS is challenging due to the overlapping of ion signals of constituents

Table 2.1 Operating modes of the TWIMS–MS instrument utilizing the TriWave™ section

Mode	TriWave™ usage			Products
	Trap	TWIMS device	Transfer	
Mobility-ToF	Ion guide only	Ion-mobility separation	Ion guide only	Ions are separated according to their mobility; drift time measurements enable collision cross-section estimations after calibration of the TWIMS device
Trap fragmentation	Elevated energy	First-generation fragment ions	Ion guide only	First-generation fragment ions are ion mobility separated
Transfer fragmentation	Storage device only	Precursor ions	Elevated energy	Precursor ions are separated according to their mobility. First-generation fragment ions align with precursor ion drift time
Time-aligned parallel (TAP) fragmentation	Elevated energy	First-generation fragment ions	Elevated energy	First-generation fragment ions are separated according to their mobilities. Activation in the transfer device results in second-generation product ions which are time-aligned to the respective first-generation product ion precursor

of the highly complex mixtures of proanthocyanidins oligo- and polymers differing in length (i.e., degree of polymerization or DP), subunit composition, and type of linkage between flavanol units [29–33].

The three-dimensionality of TWIMS–MS dataset is highlighted in Fig. 2.2a–d. ESI–TWIMS–MS driftscope images (drift time versus m/z; color coding: white most to blue least abundant ions) of a typical grape seed proanthocyanidin preparation are shown (Figs. 2.2a, c). What makes these images remarkable is (i) the separation of the ions into distinct charge state groups which are denoted as (+1) and (+2) and (ii) the separation of the proanthocyanidin oligomers into distinct ion clusters. The sodium adducts of the proanthocyanidin oligomer ions displayed shorter drift times than the corresponding protonated molecular ions (Fig. 2.2a).

In the TWIMS–MS driftscope image depicted in Fig. 2.2a, the gas-phase mobility separation of singly protonated proanthocyanidin ions from the doubly protonated proanthocyanidin ions is highlighted. The two charge state groups are denoted with (+1) and (+2). In Fig. 2.2b, a section of the ESI mass spectrum (*m/z* 500–1,400) is depicted. Singly charged ion signals dominate the mass spectrum. Due to the mobility separation of singly and doubly charged ions, it is possible to extract distinct ion clusters, which helps with the analysis of overlapping ion signals. For instance, extraction of the singly protonated ions of the procyanidin trimer (PC3, $[M+H]^+$, m/z 867.2) and the doubly protonated ions of the procyanidin hexamer (PC6, $[M+2H]^{2+}$, m/z 866.2) results in mass spectra that show baseline resolved isotope clusters (Fig. 2.2c).

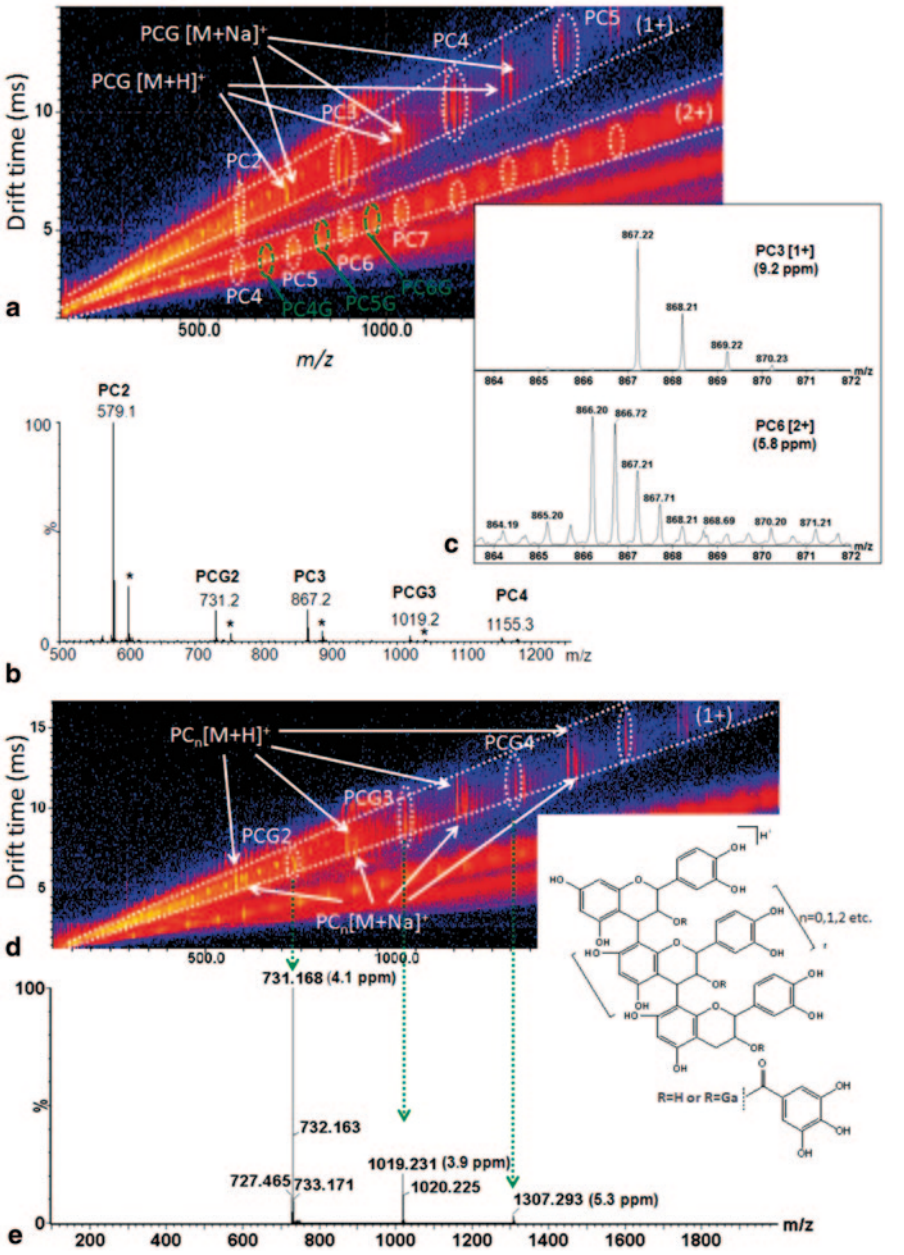

Fig. 2.2 TWIMS–MS analysis of grape seed proanthocyanidins. **a** TWIMS–MS driftscope image (drift time versus *m/z*) of a grape seed extract. PC ions separate in the TWIMS cell into charge groups labeled with (+1) and (+2) representing singly protonated and doubly protonated ions. **b** ESI mass spectrum of grape seed proanthocyanidins (depicted is range from *m/z* 500–1,450). The *asterisk* indicates the sodium adduct, $[M+Na]^+$, of the respective protonated molecular ion,

In the image depicted in Fig. 2.2d, arrows mark the singly protonated molecular ion clusters of procyanidins at *m/z* 579, 867, 1,155, and 1,443 corresponding to procyanidins with increasing degree of polymerization, namely DP2, DP3, DP4, and DP5. The sodiated molecular ions $[M+Na]^+$ are marked as well. The procyanidin monogallate ion clusters are encircled in this plot. Extraction of selected ion clusters allows the detailed analysis of ion signals that belong to a distinct proanthocyanidin series. For instance, the ion clusters of the procyanidin monogallates (PCG) were extracted and the respective mass spectrum of the extracted ion clusters is shown in Fig. 2.2b. The spectrum shows only the ion signals of procyanidin monogallates with DP2 (MH^+, *m/z* 731.17), DP3 (MH^+, *m/z* 1,019.23), and DP4 (MH^+, *m/z* 1,307.29).

Although the present TWIMS–MS spectra were obtained in the positive ionization mode, proanthocyanidins give information-rich TWIMS–MS plots in the negative mode. Matrix-assisted laser desorption ionization (MALDI)-MS analysis has been described as a powerful approach for the characterization of PC mixtures [28, 30]. Therefore, it would be interesting to see if the combination of MALDI with TWIMS–MS would further advance the analysis of these highly complex biopolymer mixtures. The above example attempts to demonstrate some of the features that TWIMS–MS offers as an analytical platform for the in-depth interrogation of proanthocyanidin preparations. We anticipate that TWIMS–MS will emerge as measurement technology for the comprehensive analysis of other biopolymers and bio-inspired plastics as well.

Experimental Details The instrument was operated in positive ionization mode with an ESI capillary voltage of 2.75 kV and a sampling cone voltage of 30 V. The other conditions were as follows: extraction cone voltage, 4.0 V; ion source temperature, 100 °C; desolvation temperature, 300 °C; desolvation gas flow rate, 500 L/h; and cone gas flow rate, 40.0 L/h. Ion-mobility separation conditions included: ion-mobility gas flow rate, 75.30 mL/min, IMS wave velocity, 542 m/s, and wave height, 40.0 V. Argon was used as collision gas in the trap and transfer cells, while nitrogen (N_2) was used as IMS cell gas. Data acquisition was carried out using Waters MassLynx (V4.1), and for IMS data processing DriftScope software (V 2.1, Waters) was used. Positive ion mass spectra were acquired in the resolution mode over a mass range of 100–2,500 *m/z* using continuum mode setting. Mass calibration in positive mode was performed by infusing sodium iodide solution (2 µg/µL, 1:1 (v/v) water:2-propanol).

$[M+H]^+$. **c** The inset shows the extracted mass spectra of the singly protonated ions of procyanidin trimers, PC3, (upper mass spectrum) and the doubly protonated ions of procyanidin hexamers, PC6 (lower mass spectrum). Note the baseline-resolved isotope cluster for the doubly protonated PC6 ions; TWIMS–MS enables the gas-phase separation of the singly protonated ions from the doubly protonated PC oligomers avoiding overlapping of the isotope clusters on the *m/z* scale. **d** Distinct ion clusters can be individually extracted and exported to display the respective mass spectra. The extracted mass spectrum depicting singly protonated procyanidin (PC_n) oligomers with DP 2–4 is shown. Sodiated proanthocyanidin ion $[M+Na]^+$ has been annotated as well. Procyanidin monogallate (PCG) ion clusters are seen in between procyanidin clusters. **e** Extracted ion signals for procyanidin monogallates

2.4 Tandem Mass Spectrometry Approaches for the Structural Analysis of Plant Phenolics Using Dried Spot Analysis in Combination with TWIMS–MS

The need for high-throughput techniques for the analysis of dietary supplements and active ingredients encouraged us to explore the combination of dried spot analysis using thin-layer chromatography (TLC) plates in combination with ESI–TWIMS–MS. A combination of TLC, desorption electrospray ionization, and TWIMS–MS has been described previously for the direct analysis of pharmaceutical formulations [34]. The combination of ion-mobility separation with MS allows gas-phase ions to be separated by their mobility and then to be analyzed according to their mass-to-charge ratio in the TOF analyzer. Analysis specificity is further increased by combining ion-mobility separation with collision-induced fragmentation in the transfer region of the Synapt G2 instrument, thus, enabling the extraction of structural information and high resolution accurate mass measurements in one experiment. The combination of TLC-based spot analyses and ESI–TWIMS–MS resembles a multidimensional separation approach that results in high-content mass spectral information for the analytes of interest. Here, we describe the application of TWIMS–MS with tandem mass spectrometry for the analysis of bioactive flavonoids in dietary supplements, namely rutin (quercetin-3-O-rutinoside, $C_{27}H_{30}O_{16}$, M_{mono} 610.1534 Da) and hesperidin (hesperitin-7-O-rutinoside, $C_{28}H_{34}O_{15}$, M_{mono} 610.1898 Da).

Dietary supplements were extracted with methanol and the extracts were spotted on cellulose TLC plates. A CAMAG TLC MS interface combined with an LC system was used for eluting the analytes from the TLC plate and subsequent infusion into the mass spectrometer. Under the experimental conditions used, this approach enabled the interrogation of dietary supplement spots for a time period of approximately 1.5 min. A typical total ion response is shown in Fig. 2.3a. By extracting all ion signals at the plateau of the total ion chromatogram, a 3D driftscope image is generated (Fig. 2.3b). Note the relatively broad ion distribution at *m/z* 611 indicating insufficient resolution to separate the protonated ions of hesperidin and rutin under the TWIMS conditions used. However, two well-separated ion signal distributions were observed for the sodiated ions, $[M+Na]^+$, of those two flavonoid glycosides (*m/z* 633). The selected ion signals with *m/z* 633 show better signal-to-noise ratios than the protonated molecules $[M+H]^+$ at *m/z* 611 (Fig. 2.3d, e). Under the TWIMS conditions used, hesperidin ($[M+Na]^+$, *m/z* 633.18) and rutin

measured under the current conditions (*m/z* range 100–1,200 Da). Note the broad ion assemblies at *m/z* 611 and the two ion distributions with similar *m/z* values at *m/z* 633 but clearly different drift time distributions. **d** and **e** Comparison of drift time distributions of ion signals observed for two over-the-counter dietary supplements that contain both flavonoid diglycosides, hesperidin ($[M+Na]$ *m/z* 633.18, dt 5.21 ms), and rutin ($[M+Na]$ *m/z* 633.14, dt 5.97 ms). Drift time distributions were obtained by selecting the ions at *m/z* 633 with the quadrupole device Q1 followed by gas-phase separation of the ions in the TWIMS cell. In **e**, the mass spectrum has a different *m/z* scale than in **d** to illustrate that the ion signals for both flavonoid diglycosides ($[M+Na]^+$) are observable at the *m/z* scale

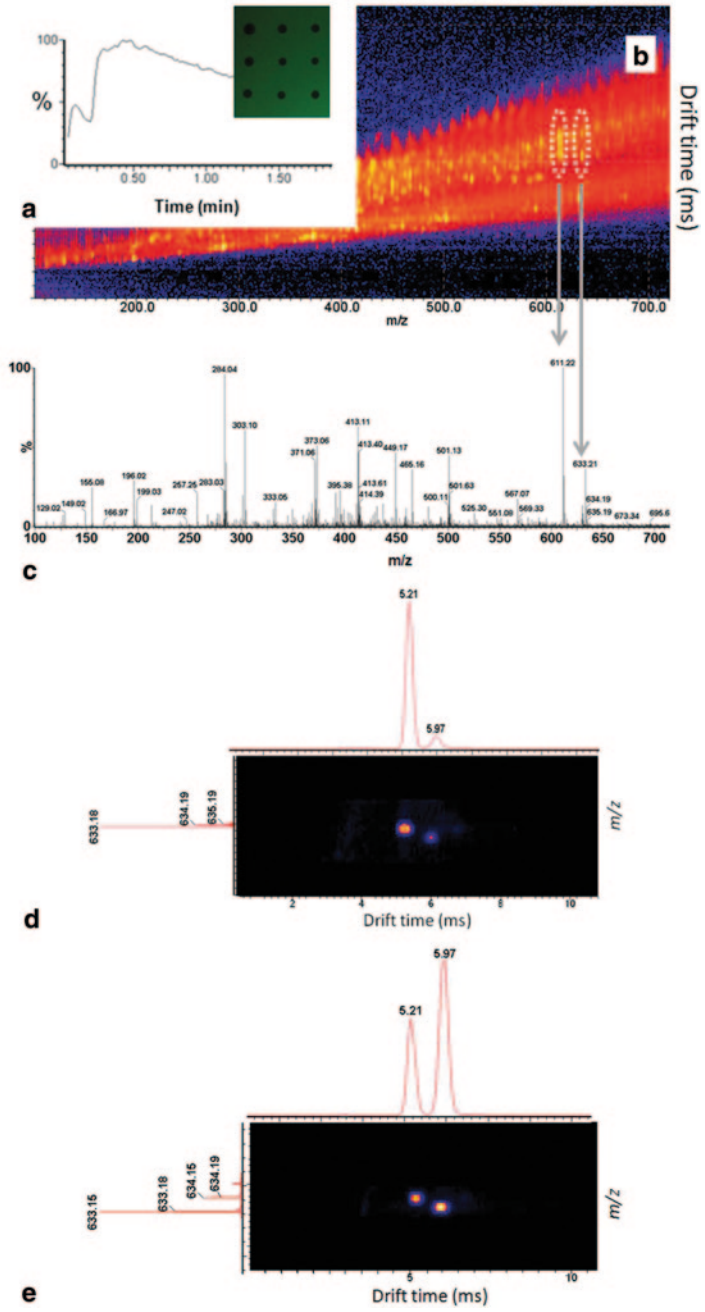

Fig. 2.3 Dried spot analysis of phytochemicals in dietary supplements with electrospray ionization TWIMS–MS. **a** Total ion chromatogram of a dietary supplement spotted on cellulose TLC plate, extracted from the plate, and infused into the mass spectrometer. **b** Driftscope image (drift time versus *m/z*) and **c** the integrated mass spectrum over the entire range of drift time distributions

($[M+Na]^+$, *m/z* 633.14) had drift time distributions centered around 5.21 and 5.97 ms, respectively.

In order to obtain structural information, the ions at *m/z* 633 were subjected to tandem mass spectrometry using the transfer region of the TriWave™ device. Transfer fragmentation was conducted by selecting the ions at *m/z* 633 using the quadrupole device. Ions were then separated in the T-wave ion-mobility cell and subsequently subjected to collision-induced fragmentation in the transfer region (Fig. 2.4a). Applying elevated collision energy to the transfer device causes fragmentation of the mobility-separated precursor ions. Because the fragment ions preserve their velocity of the precursor ion, the fragment ions align with the drift times of the precursor ions. The ions at *m/z* 633 were selected in the quadrupole region, separated in the T-wave cell, and subsequently fragmented by collisions in the transfer region. The integrated fragment ion spectrum is shown in Fig. 2.4b. In Figs. 2.5 and 2.6, the fragment ion mass spectra of the sodiated molecular ions of hesperidin and rutin are shown, respectively. The time-aligned and compound-specific ions were extracted for each of the flavonoid glycosides separately. Because transfer dissociation experiments were conducted using sodiated precursor ions, the fragment ions are sodiated as well. Fragment ions of the rutinoside moiety dominated the spectrum for both species. The observed fragment ions are indicated in the schematic presentation of the two flavonoid glycoside structures.

Experimental Details The analytes were extracted using a CAMAG TLC interface from cellulose TLC plates using 75% acetonitrile/25% water. A Shimadzu LC-10AD pump was used for solvent delivery. The flow rate was 0.1 mL/min. Mass spectral experiments were performed using a Waters Synapt G2 HDMS mass spectrometer (Manchester, UK) equipped with TWIMS. Mass spectra were acquired in positive mode. The instrument was operated in the resolution mode with a capillary voltage of 3.0 kV and a sampling cone voltage of 30.0 V. The other conditions comprise the following: extraction cone voltage, 4.1 V; ion source temperature, 80 °C; desolvation temperature, 250 °C; desolvation gas flow rate, 500 L/h; and cone gas flow rate, 5.0 L/h. Ion-mobility separation conditions included ion-mobility gas flow rate; 90 mL/min, wave velocity ramping from 480 to 556 m/s; and wave height, 40.0 V. Argon was used as collision gas on the trap and transfer cells, while nitrogen (N_2) was used as IMS cell gas. Data acquisitions were carried out using Waters MassLynx (v4.1). IMS–MS data were processed with DriftScope software (v2.1, Waters). All analyses were conducted in the positive ionization mode. Mass spectra were acquired over the mass range of 50–1,200 *m/z* in continuum mode. A 0.1 ng/μL solution of leucine enkephaline ($[M+H]+556.2771$) was infused at 5 μL/min as the reference mass (lock mass) for accurate mass measurements. Mass calibration in positive mode was performed by infusing sodium formate (5 mM, prepared in 1:1 (v/v) CH_3CN:H_2O).

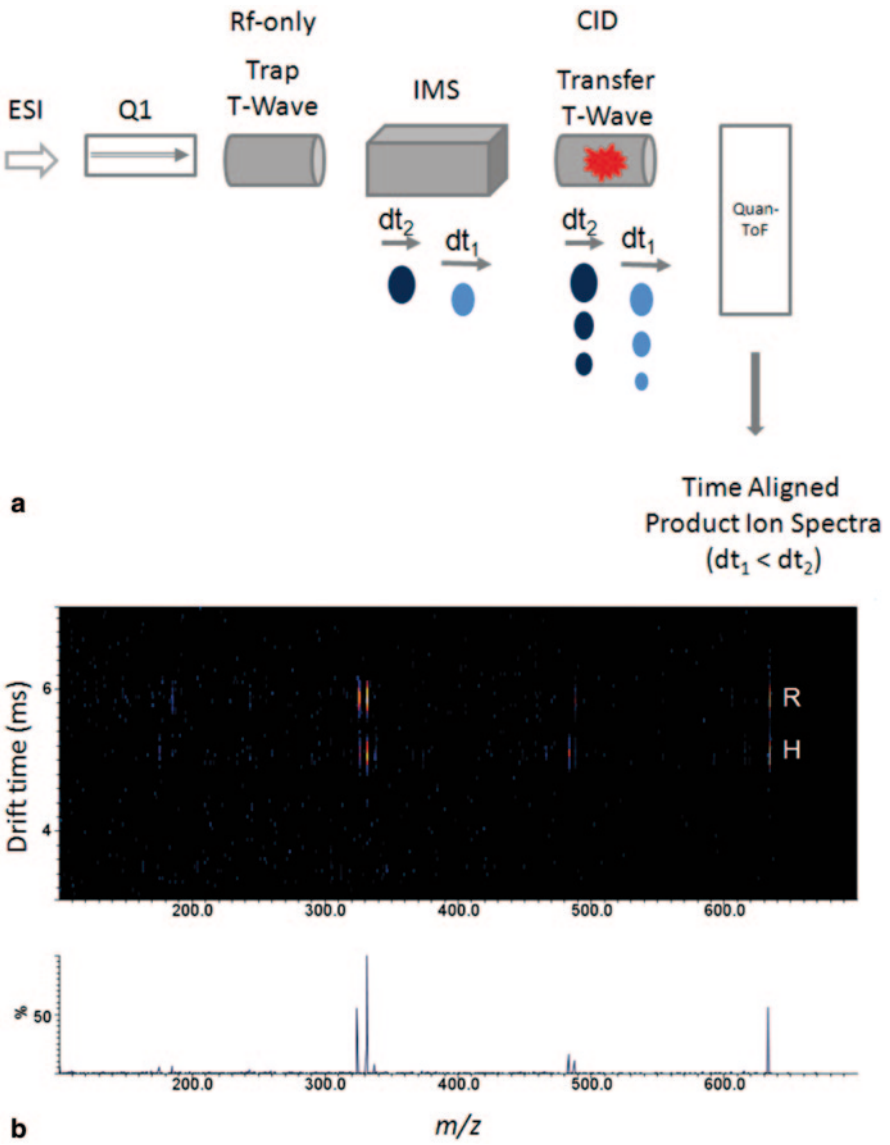

Fig. 2.4 a–b Transfer fragmentation mode for the characterization of bioactive ingredients in dietary supplements. **a** Transfer fragmentation mode—conceptual presentation. In this mode, fragment ions generated in the transfer region can be correlated to their time-aligned precursor ions. This mode of operation is particularly useful for distinguishing isobaric precursor ions as long as the precursor ions have different interaction cross sections; *v*, velocity; *dt*, drift time. **b** TWIMS–tandem mass spectrometry analysis of a supplement that contains both flavonoid glycosides, hesperidin and rutin. Transfer dissociation was conducted by selecting the ions at *m/z* 633 in the quadrupole device Q1, separation of the ions in the TWIMS region, and by collisional activation in the transfer region. *Upper panel*: drift time plot displaying the time-aligned product ions for the precursor ions with drift times 5.21 ms (hesperidin, $[M+Na]^+$) and 5.97 ms (rutin, $[M+Na]^+$). *Lower panel*: extracted tandem mass spectrum after integration of the ion signals that contribute to both time-aligned drift time distributions at 5.21 and 5.97 ms. *H*, hesperidin; *R*: rutin

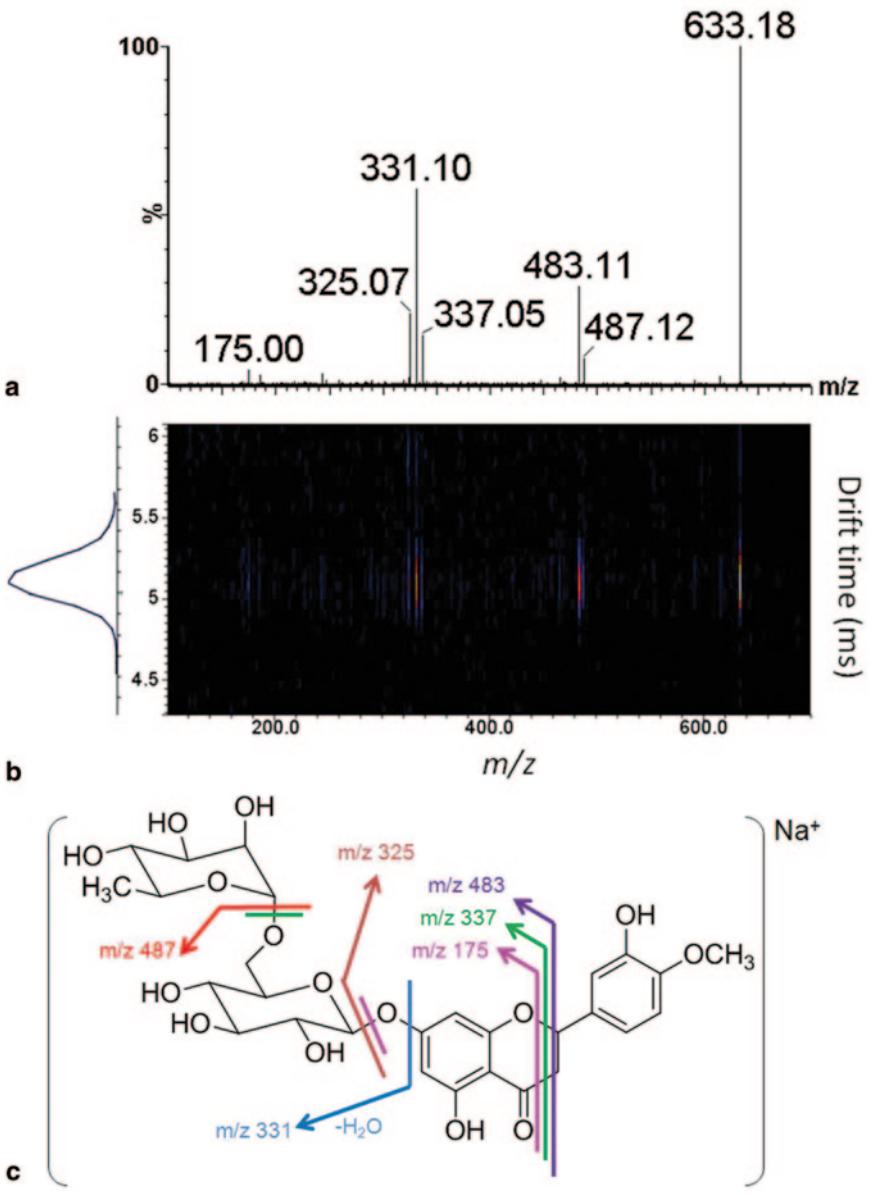

Fig. 2.5 ESI q-IMS–MS/MS transfer dissociation analysis of the sodiated hesperidin ions ($[M+Na]^+$, *m/z* 633). **a** Fragmentation spectrum, **b** drift time distribution, and **c** the proposed transfer dissociation pathways of sodiated hesperidin

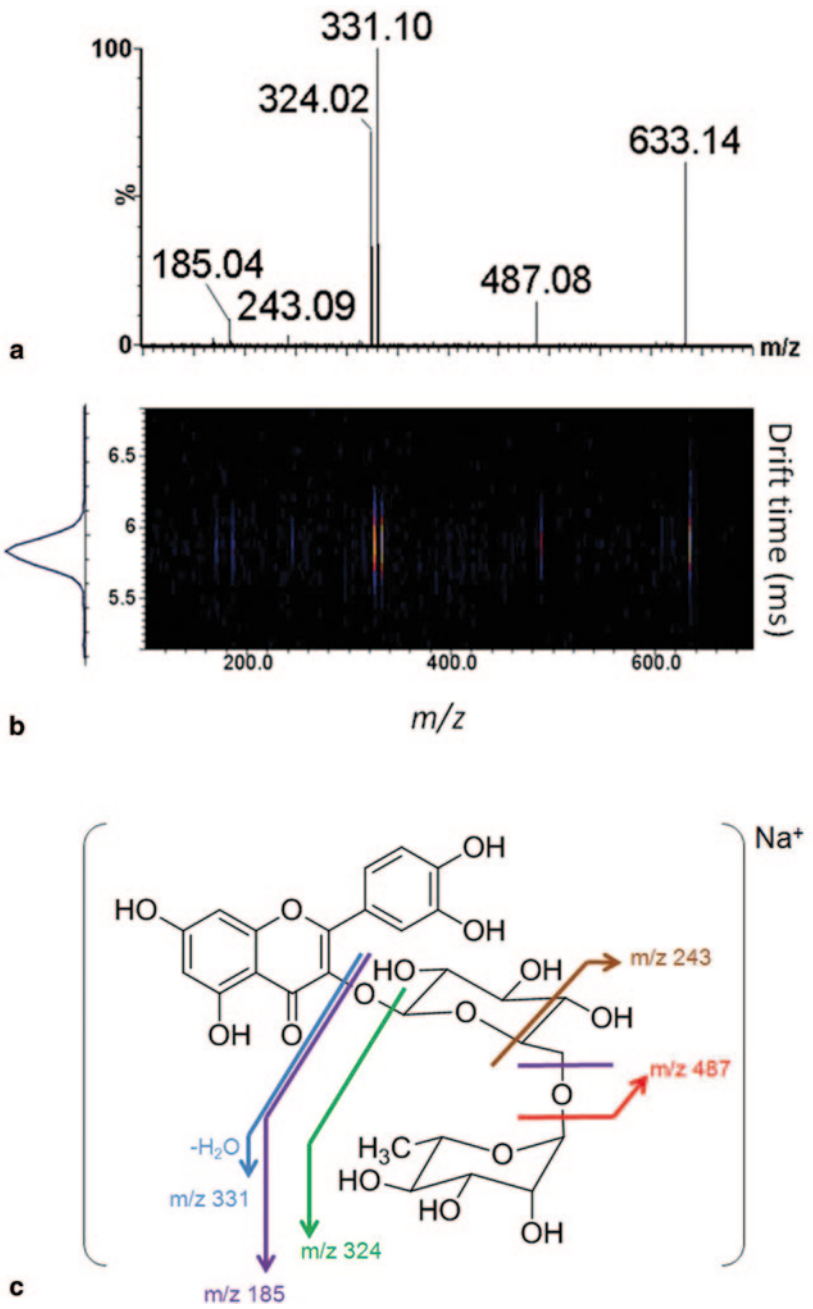

Fig. 2.6 ESI q-IMS–MS/MS transfer dissociation analysis of the sodiated rutin ions ($[M+Na]^+$, *m/z* 633). **a** Fragmentation spectrum, **b** drift time distribution, and **c** the proposed transfer dissociation pathways of sodiated rutin

2.5 TWIMS–MS for Obtaining Collision Cross Sections as an Additional Parameter for Plant Metabolite Characterization

In metabolomics, the characterization of a metabolite, e.g., a plant natural compound, is currently based on accurate mass, fragment ion spectra, and retention time comparison with a standard compound. Collision cross sections are independent of chromatographic conditions and therefore collision cross-section determinations would add an additional dimension to the characterization of a metabolite. Collision cross-section determinations have the potential of distinguishing structural isomers which is usually not possible solely by MS-based methods. We have started to build up a database for plant metabolites that compiles classical MS data (accurate mass, tandem mass spectral data) and collision cross sections. Here, we report on the determination of collision cross sections for a selection of hop phenolics. Hop phenolics have recently attracted public attention because of their health-promoting effects. These compounds show antiproliferative activity, cancer chemopreventive, and antioxidant properties [2]. Specifically, we were interested in applying TWIMS–MS for the characterization of isobaric hop phenolics, namely (i) the hop chalcone xanthohumol (XN)and the isobaric prenylated flavonoid isoxanthohumol (IX), and (ii) the two geometric isomers 6- and 8-prenylnaringenin (6-PN, 8-PN).

TWIMS separates ions according to their mobility through a continuous sequence of transient voltage pulses (traveling waves). The mobility of an ion through the T-wave cell depends on the charge on the ion, the mass of the ion and the buffer gas, the identity, temperature and pressure of the buffer gas, and its collision cross section. Hence, the collision cross section, Ω, of an ion can be expressed as given in Eq. 2.1. Since the separation of ions in the TWIMS section of the instrument is more complex than a classical drift tube, additional parameters (A and B) need to be included to account for the nonlinear effects of the TWIMS device [24, 27]:

$$\Omega = Z\,e\left[\frac{1}{m_1}+\frac{1}{m_N}\right]^{1/2} A t_D{}^{B} \tag{2.1}$$

Ω = Collision cross section
Z = Number of charges on the analyte ion
e = Charge on an electron
m_1 = Mass of the analyzed ion
m_N = Mass of the buffer gas
A = Correction factor for the electric field parameters
B = Correction factor for the nonlinear effect of the TWIMS device
t_D = Drift time

Since the separation of ions in the TWIMS section of the instrument is more complex than a classical drift tube, which uses a constant electric field, the T-wave mobility separation device needs to be calibrated. For this purpose, a drift time calibration procedure was applied that uses absolute cross-section values of polyglycine (Poly-Gly) and polyalanine (Poly-Ala) peptide ions known from classical

Table 2.2 Estimated collision cross-section values of hop phenolic compounds which were obtained by TWIMS–MS

Compound	Estimated CCS[a] (Å^2)			Theoretical CCS[a], (Å^2)
	Poly-Ala[b]	Poly-Gly[b]	Poly-Ala[b] and Poly-Gly[c]	
XN[d]	128.3	128.9	125.4	127.7
IX[e]	123.5	122.8	120.4	120.3
6-PN[f]	122.9	n.d.	120.2	118.7
8-PN[g]	119.9	n.d.	117.2	122.1

Experimentally estimated cross sections were derived by comparison with poly-DL-alanine mixture (Poly-Ala) and oligo-glycine (Poly-Gly) mixture following the procedure described by Williams et al. [32]. For comparison, theoretical cross sections are listed in the right column of the table

[a] Collision cross section
[b] Poly-DL-alanine
[c] Polyglycine
[d] Xanthohumol
[e] Isoxanthohumol
[f] 6-Prenylnaringenin
[g] 8-Prenylnaringenin

drift-tube ion-mobility studies [26, 35, 36]. The experimentally estimated cross-section values were then compared to the calculated cross sections (Table 2.2). The theoretical cross sections of the compounds were obtained by using the DriftScope software (v4.1). This software uses the projection approximation (PA) approach which is also one of the models in the MOBCAL software, a program to calculate mobilities which was developed by Martin Jarrold's group [37]. Briefly, MOBCAL calculates the collision cross-sections based on three different models. These models are the exact hard sphere scattering (EHSS), projection approximation (PA), and the trajectory model™. PA calculates cross sections in regard to a collision between the buffer gas and the analyte atoms [38–40].

XN and IX (M^-, *m/z* 353.15) were detected after TWIMS–MS in negative mode with slight difference in their drift time distributions (t_{DTD} ~0.2 ms). As shown in Fig. 2.7, infusion of the IX solution resulted always in two peaks with drift times differing by 0.2 ms. The peak ratio and drift times were the same as those detected for a mixture of IX and XN. This may indicate that isomerization of IX to XN occurred in the source prior to ion-mobility separation. A similar behavior was observed for carotenoids [15]. The isomeric PNs (M^-, *m/z* 339.12) showed distinct peaks that showed only marginally different drift time distributions under the conditions used. The experimentally estimated cross sections were in good agreement with the theoretical values. This example demonstrates that TWIMS–MS is a powerful technique that is capable of providing access to an additional analytical parameter for the in-depth characterization of phytochemicals, namely experimentally estimated collision cross sections besides exact mass determination and fragment ion information. However, more research needs to be done on structurally diverse sets of small molecules to explore the full potential and limitation of TWIMS–MS.

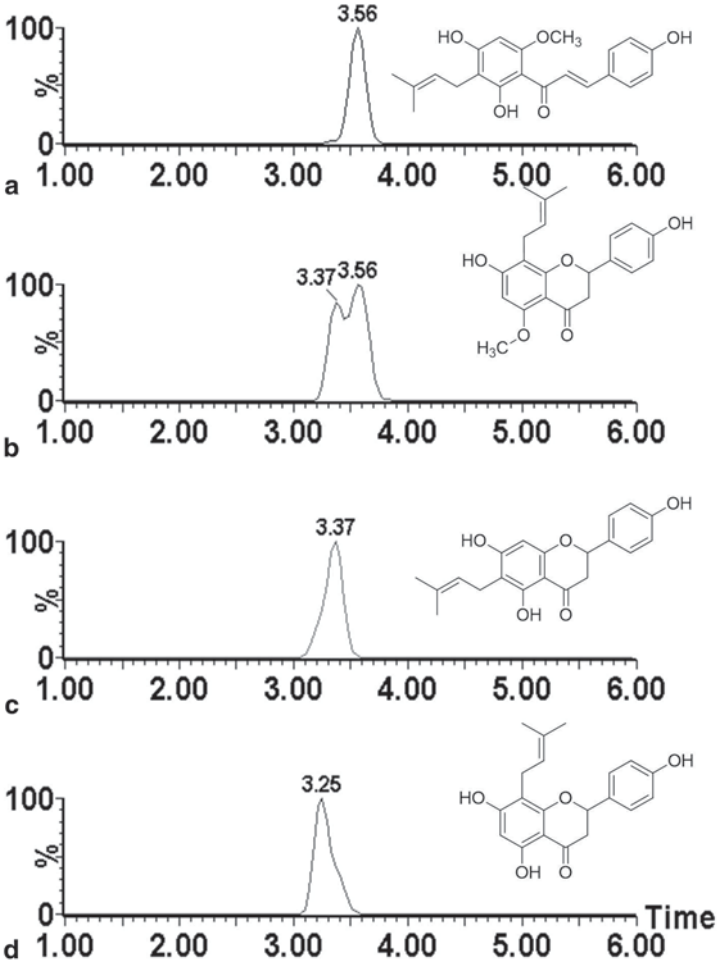

Fig. 2.7 **a**–**d** Drift time distributions and structures of the hop phenolics XN, IX, 6- and 8-PN. Negative ion electrospray TWIMS–MS analysis of the $[M-H]^-$ ions of the isomeric flavonoids XN and IX (both *m/z* 353.15, $C_{21}H_{21}O_5^-$) and the regioisomers 6- and 8-PN (*m/z* 339.12, $C_{20}H_{19}O_5^-$) was conducted following infusion. Drift time distributions were recorded for **a** XN at 3.56 ms, **b** IX at 3.37 and 3.56 ms, and **c** 6-PN at 3.37 ms and **d** 8-PN at 3.25 ms. Further work is needed to rationalize the possible isomerization of IX during the electrospray process. Calibration of the TWIMS device enables the estimation of the collision cross section (see Table 2.2). *XN*, xanthohumol; *IX*, isoxanthohumol; *6-PN*, 6-prenylnaringenin; *8-PN*, 8-prenylnaringenin; *time*, drift time in milliseconds (ms)

Experimental Details Stock solutions of XN, IX, 6-PN, and 8-PN were prepared separately (10 μg/mL) in methanol from solid standards. Equal amounts of XN and IX solutions (1:1 v/v) were mixed with 50% water before use to minimize degradation and isomerization, and then immediately infused into the ESI source at a flow rate of 5 μL/min. A solution containing both prenylated naringenins, 6-PN

and 8-PN, was prepared and infused. Mass calibrations in both modes (positive and negative) were done by infusing a solution of sodium formate (5 mM; 1:1, v/v, acetonitrile:water). The instrument was operated in the resolution mode. Source parameter settings used for negative ion acquisition were a capillary voltage of 2.0 kV and a sampling cone voltage of 25.0 V. The other optimized negative ion electrospray conditions were as follows: extraction cone voltage, 4.0 V; ion source temperature, 100 °C; desolvation temperature, 300 °C; desolvation gas flow rate, 500 L/h; and the cone gas flow was off. Ion-mobility separation settings were ion-mobility gas flow rate of 110 mL/min, wave velocity ramping from 500 to 570 m/s, and wave height of 40.0 V. Data acquisitions were carried out using Waters MassLynx (v4. 1) and ion-mobility spectra were processed using DriftScope software (v2.1, Waters).

The calibration of the T-wave cell was achieved by infusing a solution of polyalanine (Poly-Ala, 0.1 mg/mL, 1:1 acetonitrile:water) and a solution of six oligoglycines (Poly-Gly, 0.1 mg/mL in 1:1 acetonitrile:water). The flow rate was 5 µL/min. The electrospray source was operated in the positive mode and the settings were a capillary voltage of 2.25 V and a sampling cone voltage of 25 V. The ion-mobility separation conditions used for the calibration of the T-wave device were identical to those used for the analytes.

2.6 Conclusion and Perspectives

In summary, we discussed several applications of TWIMS–MS for the analysis of plant phenolics and demonstrated that combining ion-mobility separation and gas-phase fragmentation adds an extra level of selectivity and specificity for the structural characterization of plant metabolites.

We explored the use of ESI TWIMS–MS for the examination of highly complex biopolymers, namely grape seed proanthocyanidins. The use of ion-mobility separation prior to high-resolution accurate MS resulted in reduced spectral complexity compared to ESI–MS acquisitions alone. In particular, the presentation of TWIMS–MS data in a 2-dimensional contour plot, drift time vs. m/z, allows the deconvolution of many spectral features associated with the inherent heterogeneity of proanthocyanidin mixtures. We were able to extract proanthocyanidin oligomers that differ in their compositions. The capability of TWIMS–MS to separate proanthocyanidin ions with different charge groups enabled the analysis of proanthocyanidins with higher degree of polymerization compared to ESI–MS alone. There is an increasing interest in proanthocyanidins as dietary supplements, but the methods for characterizing proanthocyanidin preparations are sparse and mainly limited to gel permeation chromatography and acid hydrolysis in combination with liquid chromatography [30, 41]. Traditionally, MALDI MS has been the method of choice for the characterization of proanthocyanidin oligomers and higher-molecular-weight tannins [28, 30]. ESI–MS, in particular in combination with liquid chromatography, shows promise for the characterization of proanthocyanidins. Its broad use has been hampered by the limitation that the extraction of oligomer distribution

information is complicated due to overlapping charge state distributions of the different oligomers [30, 33]. The possible inclusion of TWIMS may provide the means to advance the analysis of proanthocyanidins. It would be interesting to evaluate MALDI TWIMS−MS for the analysis of proanthocyanidins, as it is likely that this will further improve the analysis of this class of compounds. The additional insight into the structural complexity of proanthocyanidin preparations may ultimately lead to standardized proanthocyanidin preparations for research purposes and the dietary supplements market. Beyond the current application to proanthocyanidin oligomers, IMS–MS has been used for the characterization of synthetic polymers [11, 12]. We foresee that TWIMS–MS and alternative IMS–MS techniques will significantly impact the way we characterize other biopolymers and bio-inspired polymeric materials.

TWIMS–MS technology provides access to drift time information and experimentally estimated collision cross sections, analytical parameters that are not available on MS/MS-only instruments. The potential separation and assignment of positional isomers of natural products and metabolites is an emerging application of TWIMS–MS. The potential of TWIMS of distinguishing structural isomers that differ in the site of substitutions has been proven to be a particularly powerful technique for drug metabolism studies [13, 14]. The combination of molecular modeling studies for deriving theoretically derived cross sections with TWIMS measurements of cross sections provides an exciting new strategy for the assignment of metabolite isomers. Here, an ensemble of energy-minimized metabolite structures is generated “in silico.” For the ensemble of energy-minimized structures, the theoretical cross sections are calculated. The experimentally derived cross sections are then compared with the theoretical cross sections to support the assignment of discrete metabolite structures. For instance, this approach has been successfully demonstrated for the elucidation of hydroxylation sites of ondansetron metabolites [13]. In the ondansetron metabolite study, TWIMS–MS was capable of reproducibly measuring drift time distribution differences between metabolites of 20 μs corresponding to a difference of only 0.3 Å in experimentally derived cross sections. Similarly, the capability of measuring small differences in drift times (50 μs corresponding to 0.6 Å) with TWIMS–MS was also shown for organoruthenium anticancer complexes where the arene is ortho- or meta-terphenyl [35]. Due to the increasing interest in applying TWIMS–MS characterization to small molecule studies, a small database of TWIMS-derived and validated collision cross sections for pharmaceutically relevant compounds has become available recently, which will certainly further broaden the use of TWIMS–MS for small molecule analyses [42]. Since the advent of the first commercially available TWIMS–MS instrument in 2006, technology has advanced significantly resulting in increased resolution of the traveling-wave ion-mobility separator [25], new applications [19, 43–47], and much enthusiasm in the scientific community. We foresee that TWIMS–MS and alternative IMS–MS techniques will significantly impact and advance our measuring capabilities in the phytochemical and pharmaceutical sciences, and in the emerging field of metabolomics [17, 18, 48, 49].

Advancements in system biology research will depend on tools that are capable of deconvoluting highly complex systems. The analysis of complex systems requires the availability of a new generation of separation and measurement tools. Recent applications of IMS–MS to a broad range of biomolecule measurements have demonstrated that IMS–MS has emerged as a powerful analytical technique capable of providing the separation space necessary to analyze highly complex samples [17, 23]. The combination of devices that allow real-time monitoring of living systems using IMS–MS is another exciting avenue of facilitating system-biology experiments [50]. The future for IMS–MS is bright and full of opportunities.

References

1. Tsao R (2010) Chemistry and biochemistry of dietary polyphenols. Nutrients 2:1231–1246
2. Stevens JF, Page JE (2004) Xanthohumol and related prenylflavonoids from hops and beer: to your good health! Phytochemistry 65:1317–1330
3. Miranda CL et al (2012) Flavonoids. eLS, Wiley Online Library
4. Counterman AE, Clemmer DE (2002) Cis-trans signatures of proline-containing tryptic peptides in the gas phase. Anal Chem 74:1946–1951
5. Kaleta DT, Jarrold MF (2003) Helix-turn-helix motifs in unsolvated peptides. J Am Chem Soc 125:7186–7187
6. Ruotolo BT et al (2004) Ion mobility-mass spectrometry applied to cyclic peptide analysis: conformational preferences of gramicidin S and linear analogs in the gas phase. J Am Soc Mass Spectrom 15:870–878
7. Ruotolo BT et al (2002) Observation of conserved solution-phase secondary structure in gas-phase tryptic peptides. J Am Chem Soc 124:4214–4215
8. Ruotolo BT et al (2005) Evidence for macromolecular protein rings in the absence of bulk water. Science 310:1658–1661
9. Uetrecht C et al (2010) Ion mobility mass spectrometry of proteins and protein assemblies. Chem Soc Rev 39:1633–1655
10. Zilch LW et al (2007) Folding and unfolding of helix-turn-helix motifs in the gas phase. J Am Soc Mass Spectrom 18:1239–1248
11. Trimpin S, Clemmer DE (2008) Ion mobility spectrometry/mass spectrometry snapshots for assessing the molecular compositions of complex polymeric systems. Anal Chem 80:9073–9083
12. Trimpin S et al (2007) Resolving oligomers from fully grown polymers with IMS-MS. Anal Chem 79:7965–7974
13. Dear GJ et al (2010) Sites of metabolic substitution: investigating metabolite structures utilising ion mobility and molecular modelling. Rapid Commun Mass Spectrom 24:3157–3162
14. Cuyckens F et al (2011) Product ion mobility as a promising tool for assignment of positional isomers of drug metabolites. Rapid Commun Mass Spectrom 25:3497–3503
15. Dong L et al (2010) Collision cross-section determination and tandem mass spectrometric analysis of isomeric carotenoids using electrospray ion mobility time-of-flight mass spectrometry. Anal Chem [Epub ahead of print]
16. Bohrer BC, Clemmer DE (2011) Biologically-inspired peptide reagents for enhancing IMS-MS analysis of carbohydrates. J Am Soc Mass Spectrom 22:1602–1609
17. Dwivedi P et al (2010) Metabolic profiling of human blood by high resolution ion mobility mass spectrometry (IM-MS). Int J Mass Spectrom 298:78–90

18. Castro-Perez J et al (2011) Localization of fatty acyl and double bond positions in phosphatidylcholines using a dual stage CID fragmentation coupled with ion mobility mass spectrometry. J Am Soc Mass Spectrom 22:1552–1567
19. Kliman M et al (2011) Lipid analysis and lipidomics by structurally selective ion mobility-mass spectrometry. Biochim Biophys Acta 1811:935–945
20. Kanu AB et al (2008) Ion mobility-mass spectrometry. J Mass Spectrom 43:1–22
21. Verbeck GF et al (2002) A fundamental introduction to ion mobility mass spectrometry applied to the analysis of biomolecules. J Biomol Tech 13:56–61
22. Bohrer BC et al (2008) Biomolecule analysis by ion mobility spectrometry. Annu Rev Anal Chem (Palo Alto Calif) 1:293–327
23. Liu X et al (2007) Mapping the human plasma proteome by SCX-LC-IMS-MS. J Am Soc Mass Spectrom 18:1249–1264
24. Giles K et al (2004) Applications of a travelling wave-based radio-frequency-only stacked ring ion guide. Rapid Commun Mass Spectrom 18:2401–2414
25. Giles K et al (2011) Enhancements in travelling wave ion mobility resolution. Rapid Commun Mass Spectrom 25:1559–1566
26. Michaelevski I et al (2010) T-wave ion mobility-mass spectrometry: basic experimental procedures for protein complex analysis. J Vis Exp 41: e1985
27. Smith DP KT, Campuzano I, Malham RW, Berryman JT, Radford SE, Ashcroft AE (2009) Deciphering drift time measurements from travelling wave ion mobility spectrometry-mass spectrometry studies. Eur J Mass Spectrom (Chichester Eng) 15:113–130
28. Monagas M et al (2010) MALDI-TOF MS analysis of plant proanthocyanidins. J Pharm Biomed Anal 51:358–372
29. Mouls L et al (2011) Comprehensive study of condensed tannins by ESI mass spectrometry: average degree of polymerisation and polymer distribution determination from mass spectra. Anal Bioanal Chem 400:613–623
30. Taylor AW et al (2003) Hop (*Humulus lupulus* L.) proanthocyanidins characterized by mass spectrometry, acid catalysis, and gel permeation chromatography. J Agric Food Chem 51:4101–4110
31. Porter PJ (1988) Flavans and proanthocyanidins. The Flavonoids 21–62
32. Aron PM, Kennedy JA (2008) Flavan-3-ols: nature, occurrence and biological activity. Mol Nutr Food Res 52:79–104
33. Hayasaka Y et al (2003) Characterization of proanthocyanidins in grape seeds using electrospray mass spectrometry. Rapid Commun Mass Spectrom 17:9–16
34. Harry EL et al (2009) Direct analysis of pharmaceutical formulations from non-bonded reversed-phase thin-layer chromatography plates by desorption electrospray ionisation ion mobility mass spectrometry. Rapid Commun Mass Spectrom 23:2597–2604
35. Williams JP et al (2009) Isomer separation and gas-phase configurations of organoruthenium anticancer complexes: ion mobility mass spectrometry and modeling. J Am Soc Mass Spectrom 20:1119–1122
36. http://www.indiana.edu/~clemmer/Research/Cross%20Section%20Database/Peptides/polyaminoacid_cs.htm. Accessed 14 Oct 2013
37. http://www.indiana.edu/~nano/index.html. Accessed 14 Oct 2013
38. Wyttenbach T et al (1997) Effect of the long-range potential on ion mobility measurements. J Am Soc Mass Spectrom 8:275–282
39. Ruotolo BT et al (2008) Ion mobility-mass spectrometry analysis of large protein complexes. Nat Protoc 3:1139–1152
40. Knapman TW et al. (2010) Determining the topology of virus assembly intermediates using ion mobility spectrometry-mass spectrometry. Rapid Commun Mass Spectrom 24:3033–3042
41. Kennedy JA, Jones GP (2001) Analysis of proanthocyanidin cleavage products following acid-catalysis in the presence of excess phloroglucinol. J Agric Food Chem 49:1740–1746
42. Salbo R et al (2012) Traveling-wave ion mobility mass spectrometry of protein complexes: accurate calibrated collision cross-sections of human insulin oligomers. Rapid Commun Mass Spectrom 26:1181–1193

43. Li H et al (2012) Resolving structural isomers of monosaccharide methyl glycosides using drift tube and traveling wave ion mobility mass spectrometry. Anal Chem 84:3231–3239
44. Goodwin CR et al (2012) Structural mass spectrometry: rapid methods for separation and analysis of peptide natural products. J Nat Prod 75:48–53
45. Rand K et al (2011) ETD in a traveling wave ion guide at tuned Z-spray ion source conditions allows for site-specific hydrogen/deuterium exchange measurements. J Am Soc Mass Spectrom 22:1784–1793
46. Halgand F et al (2011) Dividing to unveil protein microheterogeneities: traveling wave ion mobility study. Anal Chem 83:7306–7315
47. Ridenour WB et al (2010) Structural characterization of phospholipids and peptides directly from tissue sections by MALDI traveling-wave ion mobility-mass spectrometry. Anal Chem 82:1881–1889
48. Dwivedi P et al (2010) Metabolic profiling of *Escherichia coli* by ion mobility-mass spectrometry with MALDI ion source. J Mass Spectrom 45:1383–1393
49. Kaplan K et al (2009) Monitoring dynamic changes in lymph metabolome of fasting and fed rats by electrospray ionization-ion mobility mass spectrometry (ESI-IMMS). Anal Chem 81:7944–7953
50. Enders JR et al (2010) Towards monitoring real-time cellular response using an integrated microfluidics-matrix assisted laser desorption ionisation/nanoelectrospray ionisation-ion mobility-mass spectrometry platform. IET Systems Biology 4:416–427